ISSN 1063-7788, Physics of Atomic Nuclei, 2010, Vol. 73, No. 9, pp. 1526–1538. © Pleiades Publishing, Ltd., 2010.
Original Russian Text © S.B. Dubovichenko, 2010, published in Yadernaya Fizika, 2010, Vol. 73, No. 9, pp. 1573–1584.

NUCLEI
Theory

Astrophysical S Factors of Radiative ^{3}He^{4}He, ^{3}H^{4}He, and ^{2}H^{4}He Capture

S. B. Dubovichenko*

Fesenkov Astrophysical Institute, National Academy of Sciences of the Republic of Kazakstan, Almaty, 480068 Republic of Kazakhstan

Received October 16, 2009

Abstract—The possibility of describing the astrophysical S factors for radiative ^{3}He^{4}He capture at energies of up to 15 keV and radiative ^{3}H^{4}He and ^{2}H^{4}He capture at energies of up 5 keV is considered on the basis of the potential cluster model involving forbidden states.

DOI: 10.1134/S1063778810090073

INTRODUCTION

Radiative ^{3}He^{4}He capture at ultralow energies is of considerable interest for nuclear astrophysics since it is involved in the proton thermonuclear cycle; moreover, new experimental data on the astrophysical S factor for this process at energies of up to 90 keV and for radiative ^{3}H^{4}He capture at energies of up to 50 keV was reported in recent years. With a probability of 69%, the proton cycle may be completed with the process [1] (according to data from [2], this probability is 86%)

$$^3\mathrm{He} + {}^3\mathrm{He} \to {}^4\mathrm{He} + 2p$$

or with the reaction involving prestellar ^{4}He (which was formed after the Big Bang) and having a probability of 31% [1] (according to data from [2], this probability is about 14%),

$$^3\mathrm{He} + {}^4\mathrm{He} \to {}^7\mathrm{Be} + \gamma.$$

Moreover, the reactions of radiative ^{3}He^{4}He and ^{2}H^{4}He capture may play a nontrivial role in prestellar nucleosynthesis after the Big Bang, when the temperature of the Universe was as high as $0.3T_9$ [3].

Previously, the possibility of describing the astrophysical S factors for extremely light nuclei on the basis of the potential cluster model involving forbidden states was demonstrated by the present author in [4]. Upon the separation of orbital states according to Young's diagrams [5], this model takes into account the supermultiplet symmetry of the wave function describing the relative motion of respective clusters. The orbital-state classification used makes it possible to analyze the structure of intercluster interactions and to determine the presence and number of allowed and forbidden states in intercluster potentials and, hence, the number of nodes of the intercluster radial wave function [4].

In the present study, we calculate the astrophysical S factors for the ^{3}He^{4}He radiative-capture process at energies of up to 15 keV and the ^{3}H^{4}He and ^{2}H^{4}He radiative-capture processes at energies of up to 5 keV, relying on the potential cluster model and employing the classification of orbital states according to Young's diagrams [6] and refined values for the parameters of the ground-state potentials of the ^{7}Be, ^{7}Li, and ^{6}Li nuclei.

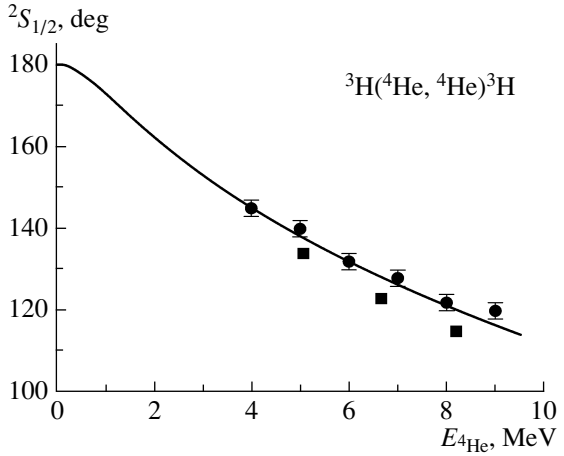

Fig. 1. $^2S_{1/2}$ phase shift for elastic ^{3}H^{4}He scattering at low energies The closed circles and boxes stand for experimental data from, respectively, [14] and [15] (the displayed errors stem from the uncertainties in determining the phase shifts from the figures in [14]). The curve represents the results of the calculations with the potential parameters from Table 1.

*E-mail: sergey@dubovichenko.ru

Table 1. Parameters of potentials for elastic ^{3}H^{4}He, ^{3}He^{4}He, and ^{2}H^{4}He scattering [11, 12] (the width parameter for ^{3}He^{4}He and ^{3}H^{4}He potential is $\alpha = 0.15747\,\text{fm}^{-2}$, while the Coulomb radius is $R_c = 3.095\,\text{fm}$)

^{7}Li, ^{7}Be			^{6}Li			
L_J	V_0, MeV	$E_{\text{FS}}(^7\text{Li})$, MeV	L_J	V_0, MeV	α, fm^{-2}	E_{FS}, MeV
$^2S_{1/2}$	−67.5	−36.0; −7.4	$^3S_1$	−76.12	0.2	−33.2
$^2P_{1/2}$	−81.92	−27.5	$^3P_0$	−68.0	0.22	−7.0
$^2P_{3/2}$	−83.83	−28.4	$^3P_1$	−79.0	0.22	−11.7
$^2D_{3/2}$	−66.0	−2.9	$^3P_2$	−85.0	0.22	−14.5
$^2D_{5/2}$	−69.0	−4.1	$^3D_1$	−63.0 (−45.0)	0.19 (0.15)	–
$F_{5/2}$	−75.9	–	$^3D_2$	−69.0 (−52.0)	0.19 (0.15)	–
$F_{7/2}$	−84.8	–	$^3D_3$	−80.88	0.19	–

POTENTIALS AND PHASE SHIFTS

As was shown in [6], the orbital states in the ^{3}He^{4}He, ^{3}H^{4}He, and ^{2}H^{4}He systems for the ^{7}Be, ^{7}Li, and ^{6}Li nuclei are pure states in Young's diagrams, in contrast to the respective states in lighter cluster systems like p^2H or p^3H [7, 8]. Therefore, potentials of the form

$$V(r) = V_0 \exp(-\alpha r^2) + V_c(r),$$

$$V_c(r) = \begin{cases} \dfrac{Z_1 Z_2}{r}, & r > R_c, \\ Z_1 Z_2 \left(3 - \dfrac{r^2}{R_c^2}\right)/(2R_c), & r < R_c, \end{cases}$$

whose parameters were fitted to phase shifts for elastic scattering can be directly used in considering properties of bound states of these nuclei in the potential cluster models [9]. In this case, the results will depend only on the degree of clustering of these nuclei in the cluster channels being considered. Since these nuclei are clustered with a comparatively high probability [5, 10], the results of the calculations are expected to reproduce, by and large, experimental data.

The values obtained in [11, 12] for the parameters of Gaussian interactions for ^{7}Li, ^{7}Be, and ^{6}Li nuclear states that are pure in Young's diagrams are listed in Table 1. The interactions in the ^{3}H^{4}He and ^{3}He^{4}He systems differ only by the Coulomb term. Table 1 presents the energies of bound forbidden states for the potentials of the ^{3}H^{4}He system, these energies differing only slightly from their counterparts for ^{3}He^{4}He interactions. Table 1 also gives the energy of the forbidden state for the ^{2}H^{4}He channel in the ^{6}Li nucleus.

In the S wave for the ^{3}H^{4}He and ^{3}He^{4}He systems, these bound states correspond to forbidden Young's diagrams {7} and {52}, while, in the P wave, they correspond to the {61} diagram in the case of the {43} allowed bound state; the D wave has a forbidden state corresponding to the {52} diagram [6, 13]. In the S wave of the ^{2}H^{4}He system, there is a forbidden bound state corresponding to the {6} diagram and an allowed bound state corresponding to the {42} diagram, while, in the P wave, the state corresponding to the {51} diagram is forbidden [6, 13].

The quality of description of the phase shifts that will be needed in the following is illustrated in Figs. 1–3 along with experimental data from [14, 15] for elastic ^{3}H^{4}He scattering, from [14, 16] for elastic ^{3}He^{4}He scattering, and from [17–20] for elastic ^{2}H^{4}He scattering. In the ^{3}He^{4}He and ^{3}H^{4}He

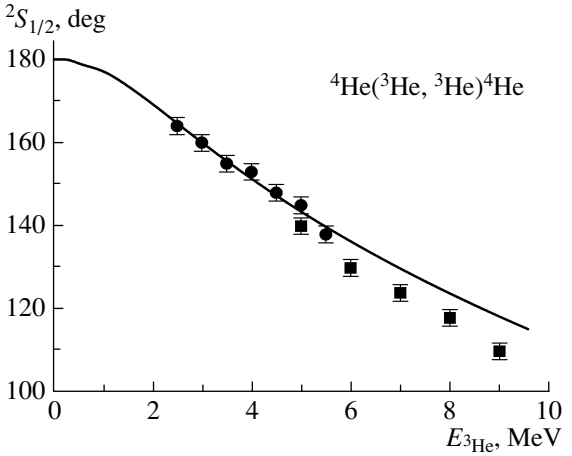

Fig. 2. $^2S_{1/2}$ phase shift for elastic ^{3}He^{4}He scattering at low energies. The closed circles and boxes stand for experimental data from, respectively, [16] and [14] (the displayed errors stem from the uncertainties in determining the phase shifts from the figures in [14, 16]). The curve represents the results of the calculations with the potential parameters from Table 1.

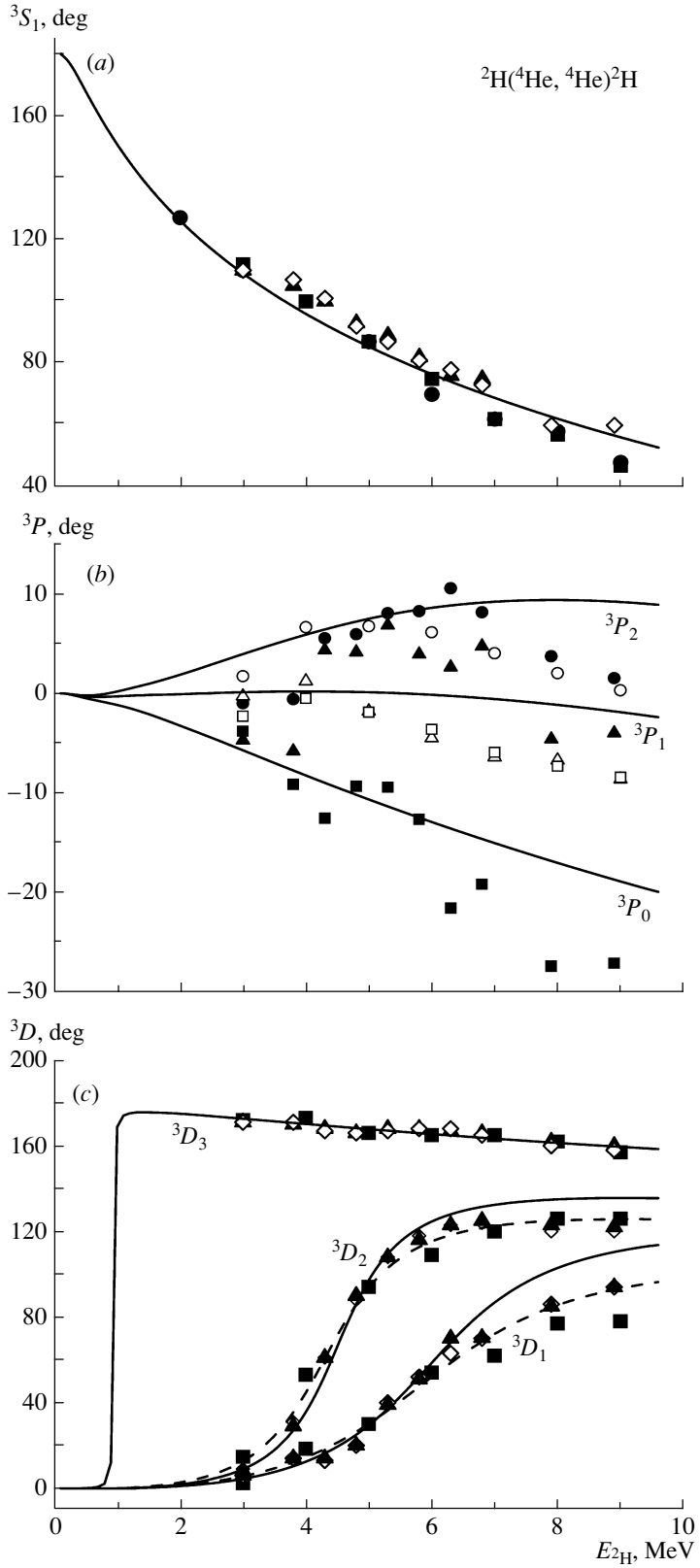

Fig. 3. Phase shifts for elastic ^{2}H^{4}He scattering at low energies: (*a*) $^3S_1$ phase shift, for which the closed circles, boxes, and triangles stand for experimental data from [17, 18, 19], while the open diamonds stand for experimental data from [20]; (*b*) ^3P phase shift, for which the open and closed circles, open and closed triangle, and open and closed boxes stand for, respectively, the P_2, P_1, and P_0 phase shifts, the open and closed symbols representing experimental data from [18] and [20], respectively; and (*c*) ^3D phase shifts, for which the closed boxes and triangles stand for experimental data from [18, 19], while the diamonds stand for experimental data from [20]. The curves represent the results of the calculations with the potential parameters from Table 1.

systems, we present only the S-wave phase shifts since, as will be shown in the following, it is the transitions from the S waves to the ground and the first excited bound state that make a dominant contribution to the astrophysical S factor for radiative capture. From Figs. 1, 2, and 3*a*, one can see that the calculated S-wave phase shifts for elastic ^{3}H^{4}He, ^{3}He^{4}He, and ^{2}H^{4}He scattering describe quite well the results of a partial-wave analysis at low energies. Figure 3*b* shows that data on the P-wave phase shifts for elastic ^{2}H^{4}He scattering from different studies are strongly different, so that one can construct P-wave potentials only approximately, but, by and large, they describe phase shifts at low energies, providing some compromise between the results of different partial-wave analysis, all calculated P-wave phase shifts being nearly coincident and being close to zero at energies below 1 MeV—that is, in the region where one considers the astrophysical S factors. In Fig. 3*c*, the results for the changed potentials that are proposed here and whose parameters are presented parenthetically in Table 1 are represented by the dashed curves, which describe somewhat better the behavior of the $^3D_1$- and $^3D_2$-wave phase shifts for ^{2}H^{4}He scattering at energies above 5 or 6 MeV.

In Figs. 1, 2, and 3*a*, the S-wave phase shifts at zero energy are reckoned from 180°, even though, in the presence of two bound (allowed or forbidden) states in all systems, they must issue from 360° according to the generalized Levinson theorem [6]. Figure 3*b* shows the P-wave phase shifts for ^{2}H^{4}He scattering at zero energy from 0°, even though, in the presence of a bound forbidden state corresponding to the {51} diagram, they must issue from 180°.

Further, the intercluster interactions matched in this way with the phase shifts were used to calculate various properties of the ground state of the ^{7}Li, ^{7}Be, and ^{6}Li nuclei and of electromagnetic processes in these nuclei, and specific properties of corresponding nuclei in a free state were associated with clusters [11–13]. The parameters of the potentials for the bound states in the P wave for the ^{3}He^{4}He and ^{3}H^{4}He systems and in the S wave for the ^{2}H^{4}He system were fixed predominantly on the basis of a fit to the binding energy [13]. In the last case, it was possible to reproduce not only the binding energy but also the behavior of the S-wave phase shift for elastic scattering (Fig. 3*a*) at low energies, all of these results being obtained without allowing for tensor forces [21].

Fairly good agreement between the results of the calculations and various experimental data was obtained within this approach both for electromagnetic processes and for basic properties of bound states of many light nuclei in cluster channels [6, 13].

NEW VERSIONS OF POTENTIALS

Previously, the binding energy of the ^{7}Li nucleus in the $J = 3/2^-$ ^{3}H^{4}He channel was actually determined, in just the same way as in the case of other systems, to a precision of several keV units; therefore, the accuracy in determining the astrophysical S factor for radiative capture proved to be relatively low even at 10 keV. In the present study, we refine basic calculated features of bound states of the ^{7}Li, ^{7}Be, and ^{6}Li nuclei in the ^{3}H^{4}He, ^{3}He^{4}He, and ^{2}H^{4}He channels. For this, we refine the parameters of the potentials for the bound states. We present these refined parameters in Table 2, along with the calculated energy levels, which are in perfect agreement with their experimental counterparts [22]. In the case in question, the potential parameters were chosen in such a way as to describe precisely the measured energy levels. If the experimental binding energy [22] was known to the fourth decimal place inclusive after the decimal point—for example, −1.4743 MeV—it was assumed that this energy can be written to the sixth decimal place, −1.474300 MeV. The energies of bound-state levels in the nuclei under consideration for preset potentials were calculated by the finite-difference method [23] to a precision not poorer that 10^{-6} MeV (1 eV). In the following, we will show that the actual accuracy in determining the binding energy in all systems by two different methods proves to be at a level of ±1 eV. In all probability, the largest error is likely to be introduced by the second, variational, method, which involves expanding the wave function in a nonorthogal Gaussian basis and independently varying parameters [23].

So small a change in the parameters of the ^{3}H^{4}He, ^{3}He^{4}He, and ^{2}H^{4}He potentials in Table 2 in relation to the results reported in [9, 13] and presented in Table 1 has virtually no effect on the behavior of phase shifts. However, this change makes it possible to reproduce the energy of levels in cluster channels to the highest possible precision, and this plays a significant role in calculating the astrophysical S factors for energies of about 1 to 10 keV. There is now (see Table 2) a small distinction between the parameters of the ^{3}H^{4}He and ^{3}He^{4}He potentials, which is required for more precisely describing channel energies.

The potential widths in Tables 1 and 2 were chosen in such a way as to attain a reasonable description of charge radii and asymptotic constants [13]. Table 2 gives the results obtained by calculating the charge radii of the nuclei under consideration in cluster channels. In order to determine the charge radius of a nucleus, we employed the cluster radii that were presented in [22, 24, 25] and whose values are given in Table 3 along with the energies of bound states in cluster channels and cluster masses. In the presence

Table 2. Refined parameters of the bound-state potentials for the ^{3}H^{4}He, ^{3}He^{4}He, and ^{2}H^{4}He interactions and energy levels and charge radii calculated with these parameters for the ^{7}Li, ^{7}Be, and ^{6}Li nuclei (for the ^{3}H^{4}He and ^{3}He^{4}He systems, $\alpha = 0.15747\,\text{fm}^{-2}$ and $R_c = 3.095\,\text{fm}$)

^{7}Li				^{7}Be		
L_J	V_0, MeV	E, MeV	$\langle r^2\rangle^{1/2}$, fm	V_0, MeV	E, MeV	$\langle r^2\rangle^{1/2}$, fm
$^2P_{3/2}$	−83.616808	−2.467000	2.46	−83.589554	−1.586600	2.64
$^2P_{1/2}$	−81.708413	−1.990390	2.50	−81.815179	−1.160820	2.69

^{6}Li				
L	V_0, MeV	α, fm^{-2}	E, MeV	$\langle r^2\rangle^{1/2}$, fm
$^3S_1$	−75.8469155	0.2	1.474300	2.65

Table 3. Experimental data on charge radii, cluster masses, and binding energies [22, 24, 25]

Nucleus	Radius, fm	Mass and energy
^{2}H	2.1402(28)	2.013553212724 amu
^{3}H	1.63(3); 1.76(4); 1.81(5)	3.0155007134 amu
	Average 1.73	
^{3}He	1.976(15); 1.93(3); 1.877(19); 1.935(30)	3.0149322473 amu
	Average 1.93	
^{4}He	1.671(14)	4.001506179127 amu
^{6}Li	2.51(10)	$E_{^4\text{He}^2\text{H}} = -1.4743$ MeV
^{7}Li	2.35(10)	$E_{^4\text{He}^3\text{H}} = -2.467\,(3/2^-); -1.99039\,(1/2^-)$ MeV
^{7}Be	–	$E_{^4\text{He}^3\text{He}} = -1.5866\,(3/2^-); -1.16082\,(1/2^-)$ MeV

of several different experimental results, we took their average value.

From Table 2, one can see that the calculated root-mean-square radius of the ^{7}Li nucleus proves to be somewhat larger than the experimental value presented in Table 3. This may be due to the experimental uncertainty that is present in the cluster radii (Table 3), which may be as large as ±5% of the average value, and which may change the radius of the nucleus by 0.05 fm. For the ^{6}Li nucleus, it is common practice to assume that the deuteron must have a deformed shape within the nucleus, and this makes it possible to explain a somewhat overestimated radius [9]. In this way, not only can one faithfully reproduce the energies of levels, but it is also possible to obtain quite acceptable values for charge radii with such potentials. By and large, these values agree with experimental data.

In order to test the stability of the tail of the wave functions for the ground and first excited states at large distances, use was made of the asymptotic constant C_w, which was represented in the form [26]

$$\chi_L = \sqrt{2k_0}C_w W_{\eta L}(2k_0 r),$$

where χ_L is the numerical wave function that is obtained for the bound state by solving the radial Schrödinger equation and which is normalized to unity; W is the Whittaker function describing a bound state, determining the asymptotic behavior of the wave function, and appearing to be a solution to the same equation but without a nuclear potential—that is, a solution at long distances; k_0 is the wave number associated with the channel binding energy; η is the Coulomb parameter; and L is the orbital angular momentum of a bound state.

As a result, the following values of the asymptotic constants were obtained for the ground states of the ^{7}Be, ^{7}Li, and ^{6}Li nuclei in the channels being considered: 5.03(1), 3.92(1), and 3.22(1) for the first, second, and third ones, respectively. For the first excited states of the ^{7}Be and ^{7}Li nuclei, the values of 4.64(1) and 3.43(1), respectively, were found within

this model. The quoted error is determined by the averaging of the constant obtained from the calculation over the interval 6–16 fm for the ^{7}Be and ^{7}Li nuclei and over the interval 5–19 fm for the ^{6}Li nucleus.

The value of 2.71 for the asymptotic constant characterizing the S-wave ground state of the ^{6}Li nucleus in the ^{2}H^{4}He channel was obtained in [27] on the basis of the three-body np^4He model. The value of 2.93(15) was found in [28] from an analysis of the phase shifts for elastic ^{2}H^{4}He scattering. Values of the constant between 1.64 and 2.78 were obtained in [29] for various types of NN and $N\alpha$ interactions. In [29], there are references to experimental data leading to asymptotic-constant values between 2.29(20) and 2.32(11). If the asymptotic constant is determined for ^{2}H^{4}He from the ordinary exponential asymptotic behavior (that is, without allowance for Coulomb effects), its value within the model used is 1.9(2) over the interval 4–12 fm. The following values of the asymptotic constants are known for the case in question: 2.4 [30] and 2.15(5) [26, 31].

A survey of asymptotic and vertex constants, including those for the ^{2}H^{4}He channel, was given in [32], and it was indicated there that, depending on the presence or absence of Coulomb effects, their values may differ severalfold. Actually, the asymptotic constant in the results presented above changes from 1.64 to 2.93—that is, nearly by a factor of two.

In [33], for example, values of the asymptotic constant in the range 3.54–3.83 were obtained for the ground state of the ^{3}H^{4}He system in the ^{7}Li nucleus by using the asymptotic behavior in the Whittaker form, which takes into account Coulomb effects, while, in [34], the value of 3.55(28) was found. For the ground state of the ^{7}Be nucleus, the analysis of various experimental data in [35] led to the value of 4.82(14) in the ^{3}He^{4}He channel. Thereby, the results obtained in those studies give sufficient grounds to conclude that the values that we found for the asymptotic constants are overestimated by about 5% for the ^{7}Be nucleus and by about 10% for the ^{7}Li nucleus.

We note that the results themselves obtained for the asymptotic constants in different studies on the basis of different methods (for an overview on the subject, see [33, 35]) may differ by 30 to 50%.

VARIATIONAL RESULTS

In order to test the accuracy in determining the binding energy in the cluster systems being considered, we employe the variational method in the version that the present author proposed in [23] and which, in the ^{3}H^{4}He channel, made it possible to obtain the binding energy of −2.466998 MeV by using a nonorthogonal Gaussian basis of dimension as low as ten. Since the variational energy decreases as the dimension of the variational basis increases, providing an upper limit on the true binding energy, and since the finite-difference energy increases with decreasing step width and with increasing number of steps, we can take an average value of −2.466999(1) MeV for the actual binding energy in the potential being considered.

The expansion parameters for the radial intercluster wave function of the form [9]

$$\Phi_L(R) = R^L \sum_i C_i \exp(-\alpha_i R^2)$$

for the ^{3}H^{4}He system are given in Table 4. The asymptotic constant C_w was at a level of 3.93(3) at distances in the range 6–16 fm, and the residual value did not exceed 3×10^{-12} [23]. For the first excited bound state in the ^{3}H^{4}He channel, we obtained the energy of −1.990374 MeV. The respective wavefunction parameters are also given in Table 4. The asymptotic normalization constant in the interval 6–20 fm proved to be 3.40(5), and the residual value did not exceed 4×10^{-13}.

For the binding energy in the ^{3}He^{4}He channel, the value of−1.586598 MeV was obtained by using a ten-dimensional basis; the respective expansion coefficients for the wave function are given in Table 5. On the basis of these results, it can be concluded that the value of −1.586699(1) MeV can be taken for the average binding energy in the potential being considered. The asymptotic normalization constant is at a level of 5.01(4) in the range 6–15 fm, and the residual value does not exceed 5×10^{-13}. The energy of −1.160801 MeV was obtained for the first excited state in the ^{3}H^{4}He channel, and the respective wavefunction parameters are also given in Table 5. The asymptotic normalization constant in the range 6–14 fm proved to be 4.64(4), and the residual values were less than 5×10^{-12}.

In the ^{2}H^{4}He channel, the variational method leads to the energy of −1.474298 MeV, so that the average binding energy in the potential being considered is −1.474299(1) MeV. The asymptotic normalization constant in the range 6–20 fm is 3.23(3), and the residual value does not exceed 7×10^{-13}. The expansion parameters for the variational wave function are given in Table 6.

Thus, we can see that, for all systems considered here, the actual difference in the ground-state binding energies found by the two methods in question does not exceed 2 eV and that the asymptotic normalization constants in the regions specified above are in perfect agreement within the quoted errors. For the charge radii obtained by the two methods, there is

Table 4. Parameters and expansion coefficients in variational wave functions for the ^{7}Li nucleus within the ^{3}H^{4}He model

^{7}Li (^{3}H^{4}He), $J = 3/2^-$, the normalization factor in the wave function over the interval 0–25 fm is N = 9.99999999992E-001		
i	α_i	C_i
1	6.567905679421632E-001	4.270672892119584E-001
2	1.849427298619411E-002	−6.326508826973404E-004
3	1.729324040753008E-001	−2.047665503330138E-001
4	4.173925751998056E-002	−1.032337189461229E-002
5	8.818471551829664E-002	−6.301223045259621E-002
6	4.503350223878621E-001	6.962475101962766E-001
7	9.210585557350788E-001	2.076348167318741E-002
8	2.000570770210328	1.488688664230068E-003
9	2.925234985697186	−1.124699482527892E-003
10	3.981951253509630	3.797289741762020E-004
^{7}Li (^{3}H^{4}He), $J = 1/2^-$, the normalization factor in the wave function over the interval 0–25 fm is N = 9.999999994E-001		
i	α_i	C_i
1	3.767783843541890E-001	4.630588198830661E-001
2	3.862289845123266E-002	−1.122717538276013E-002
3	1.902467043551489E-001	−2.185424962074149E-001
4	1.465702154047247E-002	−4.355239784992325E-004
5	9.174545622012323E-002	−7.860947071320935E-002
6	8.478055592043516E-001	−5.602419628674884E-001
7	6.512974681188465E-001	1.017849119474616
8	1.401572634787409	57.704730892399640
9	1.405534176137368	−58.402969632676760
10	1.569682720436807	9.151457061882704E-001

also agreement to the second decimal place after the decimal point for all systems considered here. These results are indicative of good agreement in the range 16–20 fm between the bound-state wave functions obtained by the two methods for all nuclei considered in the present study.

In all of these calculations, performed by finite-difference and variational methods, the numerical or variational wave function was replaced at the end of the stabilization region (that is, after 16 to 20 fm) by the Whittaker function with allowance for the value of the asymptotic normalization function. In all matrix elements, numerical integration was performed over a region extending up to 30 fm. This was done on the basis of Simpson's rule, which shows good results for smooth slowly oscillating functions [23].

In order to perform the calculations reported in this article, the computer code developed by the present author and based on the finite-difference method was refined. This made it possible to improve substantially the speed and accuracy of all calculations and to obtain, for example, more accurate values for the binding energy of a nucleus in the two-body channel. The absolute accuracy in seeking bound-state energies, for example, for the ^{3}H^{4}He system in the ^{7}Li nucleus is 10^{-6} MeV (1 eV). The accuracy in seeking a zero of the determinant that determines the accuracy in determining the binding energy is now not poorer than 10^{-15}. The Wronskians of Coulomb functions that determine the accuracy in seeking phase shifts for elastic scattering are at a level of 10^{-20} to 10^{-15} [23].

Table 5. Parameters and expansion coefficients in variational wave functions for the ^{7}Be nucleus within ^{3}He^{4}He model

^{7}Be (^{3}He^{4}He), $J = 3/2^-$, the normalization factor in the wave function over the interval 0–25 fm is $N = 9.9999999995$E-001		
i	α_i	C_i
1	7.592678086347688E-001	4.226683168050651E-001
2	1.764646518442939E-002	−9.297447488403448E-004
3	1.713620418679277E-001	−1.913577297864284E-001
4	4.166190335743666E-002	−1.157464906616252E-002
5	8.829356096205253E-002	−6.210954724479718E-002
6	4.566882349965201E-001	7.725352747968277E-001
7	1.263871984172901	−7.575809619184885E-001
8	1.358053110884124	7.836457309371079E-001
9	1.741955980844547	−1.277551712466414E-001
10	2.379459759640717	1.446300395173141E-002
^{7}Be (^{3}He^{4}He), $J = 1/2^-$, the normalization factor in the wave function over the interval 0–25 fm is $N = 9.99999998$E-001		
i	α_i	C_i
1	3.857719633413334E-001	4.891511738383773E-001
2	3.862289845123266E-002	−1.229249560611409E-002
3	1.881845128735454E-001	−2.002401467853206E-001
4	1.465702154047247E-002	−7.752125472489987E-004
5	9.174545622012323E-002	−7.680363457361430E-002
6	8.478055592043516E-001	−3.264723437643782E-001
7	6.512974681188465E-001	8.230628856230295E-001
8	1.401572634787409	21.258288548024340
9	1.405534176137368	−21.437482795337960
10	1.569682720436807	2.883954334066227E-001

The variational code was also rewritten. This made it possible to improve substantially the speed of the search for the minimum of the multiparameter functional determining the binding energy of two-body systems in all cluster channels of the nuclei considered here [23].

In all calculations, we introduced precise values of the particle masses [25] and set the constant $\hbar^2/m_0$ to 41.4686 MeV fm^2. The Coulomb parameter $\eta = \mu Z_1 Z_2 e^2/(q\hbar^2)$ was represented in the form $\eta = 3.44476 \times 10^{-2} Z_1 Z_2 \mu/q$, where q in the wave number (in fm^{-1} units) determined by the energy of interacting particles in the entrance channel, μ is their reduced mass in atomic mass units (amu), and Z stands for particle charges in units of an elementary charge e. The Coulomb potential at $R_c = 0$ was taken in the form $V_c\,(\mathrm{MeV}) = 1.439975 Z_1 Z_2/r$, where r is the distance between the input-channel particles in fm units and Z stands for particle charges in units of e.

ASTROPHYSICAL S FACTORS

Previously, the total cross sections for photoprocesses and astrophysical S factors for the ^{2}H^{4}He, ^{3}H^{4}He, and ^{3}He^{4}He systems were calculated on the basis of the cluster model [36] similar to that used here and on the basis of the resonating-group method [37]. For interactions involving forbidden states, the total photodisintegration cross sections for the ^{2}H^{4}He cluster channel of the ^{6}Li nucleus were calculated on

Table 6. Parameters and expansion coefficients in variational wave functions for the ^{6}Li nucleus within the ^{2}H^{4}He model (the normalization factor in the wave function over the interval 0–25 fm is $N = 9.99999865$E-001)

^{6}Li (^{2}H^{4}He), $J = 1^+$		
i	α_i	C_i
1	9.437818606389059E-003	5.095342831090755E-003
2	2.339033265895747E-002	3.991949900002217E-002
3	5.360473343158653E-002	1.164934149242748E-001
4	1.140512295822141E-001	2.165501771045687E-001
5	2.076705835662333E-001	1.831336962855912E-001
6	3.702254820081791E-001	−6.350857624465279E-001
7	2.848601430685521	2.165544802826948E-002
8	5.859924777191484E-001	−7.358532868463539E-001
9	82.336677993239830	5.086893578426774E-003
10	12.344385769445580	1.002621348014230E-002

the basis of three-body ground-state wave functions [38]. Within two-cluster models involving forbidden states and relying on Gaussian potentials matched with phase shifts for elastic scattering, the total cross sections for photoprocesses were calculated in [11, 13] for the ^{6}Li and ^{7}Li nuclei.

In view of the appearance of new experimental data, the astrophysical S factors in the ^{3}H^{4}He, ^{3}He^{4}He, and ^{2}H^{4}He channels are considered here at maximally low energies on the basis of the potential cluster model [11, 13] and refined potentials for the ground states of the ^{7}Li, ^{7}Be and ^{6}Li nuclei (see Table 2). In the calculations for the ^{3}H^{4}He and ^{3}He^{4}He systems, we take into account only $E1$ transitions, since the contributions of $E2$ and $M1$ processes prove to be two to three orders of magnitude smaller [3]. In these systems, there can occur an $E1$ transition between the ground ($P_{3/2}$) states of the ^{7}Li and ^{7}Be nuclei and the $S_{1/2}$, $D_{3/2}$, and $D_{5/2}$ scattering states, as well as between the first excited bound ($P_{1/2}$) state and the $S_{1/2}$ and $D_{3/2}$ waves of the continuum.

For radiative capture in the ^{2}H^{4}He channel of the ^{6}Li nucleus, $E1$ transitions from scattering P waves to the ground bound (S-wave) state of ^{6}Li and $E2$ transitions from scattering D waves to the ground state are possible. A dominant contribution to the $E2$ process at low energies comes from the $^3D_3$ wave, which has a resonance at 0.71 MeV. As for the $E1$ transition, it proves to be strongly suppressed because of the cluster factor $A_J(K)$, which is specified below, so that the radiative-capture cross section is determined primarily by the $E2$ transition. But it was shown earlier [13] that, at extremely low energies of about 100 to 150 keV, the contribution of the $E1$ transition becomes dominant; therefore, it is the $E1$ process that determines the behavior of the astrophysical S factor in this energy region, as will be seen below.

In calculating the astrophysical S factor, we used the well-known expression [39]

$$S(EJ) = \sigma(EJ)E_{\text{c.m.}} \exp\left(\frac{31.335 Z_1 Z_2 \sqrt{\mu}}{\sqrt{E_{\text{c.m.}}}}\right),$$

where σ is the total radiative-capture cross section in barns, $E_{\text{c.m.}}$ is the c.m. energy of the entrance-channel particles in keV units, μ is the reduced mass of these particles in amu, and Z stands for particle charges in elementary-charge units. The numerical coefficient 31.335 was obtained here on the basis of the present-day values of fundamental constants from [40].

The total radiative-capture cross section $\sigma(EJ)$ within the potential cluster model has the form (see, for example, [41] or [9, 13])

$$\sigma(E) = \sum_{J,J_f} \sigma(EJ, J_f),$$

$$\sigma(EJ, J_f) = \frac{8\pi K e^2}{\hbar^2 q^3} \frac{\mu}{(2S_1+1)(2S_2+1)}$$

$$\times \frac{J+1}{J[(2J+1)!!]^2} A_j^2(K) \sum_{L_i,J_i} |P_J(EJ, J_f) I_J|^2,$$

where, for $EJ(L)$ orbital electric transitions, we have the following simple expression [9, 13, 41]:

$$P_J(EJ, J_f) = \delta_{S_i S_f} (-1)^{J_i + S + L_f + J}$$

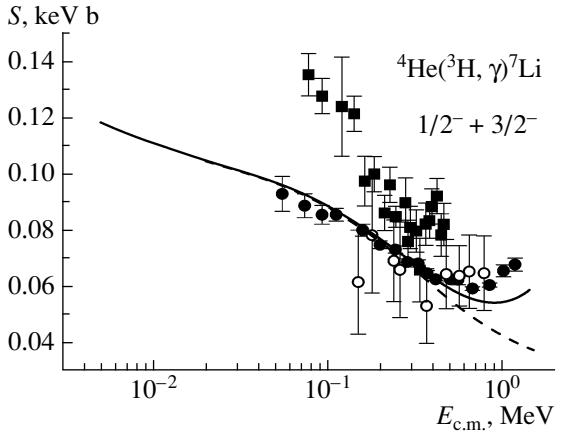

Fig. 4. Astrophysical S factor for ^{3}H^{4}He capture. The closed circles, open circles, and closed boxes stand for experimental data from [42], [43], and [44], respectively. The curves represent the results of the calculations with the parameters of the potentials for the ground states from Table 2.

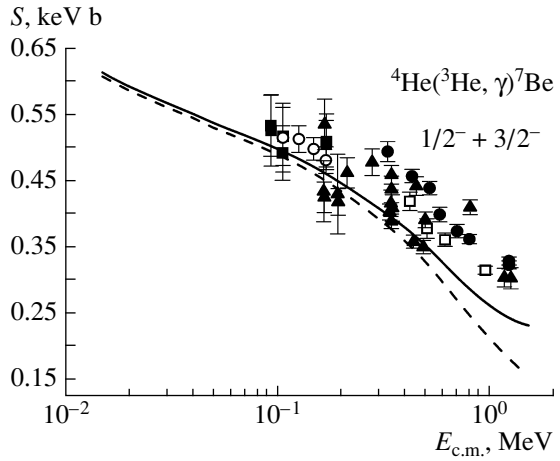

Fig. 5. Astrophysical S factor for ^{3}He^{4}He capture. The closed circles, closed boxes, open circles, open boxes, and closed triangles stand for experimental data from [45], [46], [47], [48], and [49], respectively. The curves represent the results of the calculations with the parameters of the potentials for the ground states from Table 2.

$$\times \sqrt{(2J+1)(2L_i+1)(2J_i+1)(2J_f+1)}$$

$$\times (L_i 0 J 0 | L_f 0) \begin{Bmatrix} L_i & S & J_i \\ J_f & J & L_f \end{Bmatrix},$$

$$A_J(K) = K^J \mu^J \left(\frac{Z_1}{M_1^J} + (-1)^J \frac{Z_2}{M_2^J} \right),$$

$$I_J = \langle L_f J_f | \, R^J \, | L_i J_i \rangle .$$

Here, μ is the reduced mass; q is the wave number of the entrance-channel particles; L_f and L_i (J_f and J_i) are, respectively, final- and initial-state (or, equivalently, exit- and entrance-channel) orbital (total) momenta; S_1 and S_2 are the spins of the entrance-channel particles, M_1 and M_2 are their masses, and Z_1 and Z_2 are their charges; K^J and J are the photon wave number and angular momentum, respectively; and I_J is the integral of the initial- and final-state wave functions with respect to the intercluster distance R. One sometimes includes the final-state spectroscopic factor S_{Jf} in the above expressions for the cross sections, but it is equal to unity within the potential cluster model used, as was adopted in [41].

In Fig. 4, the astrophysical S factor calculated for ^{3}H^{4}He radiative capture at energies of up to 5 keV are represented by the solid curve. The displayed experimental data were borrowed from [42, 43]. The results at energies of up to 55 keV were presented in the first of those articles. The S-factor value at 10 keV proved to be 111.0 eV b, the value extracted at zero energy from experimental data being 106.7(4) eV b [42]. Earlier results from [43] lead to the value of 64 eV b, but the errors in the data from [43] are so large that these data were extrapolated by using a straight line. There are also different data that, at zero energy, lead to the values of 140(20) eV b [44] and 100(20) eV b [41].

If we take into account only transitions from scattering S waves—that is, if we disregard transitions from D waves to the ground and first excited bound P-wave states—then, at 10 keV, there arises the S-factor value of 110.8 eV b, which is nearly identical to that which was quoted above. The results obtained by calculating the S factor as such for this case are represented by the dashed curve in Fig. 4, and this curve is seen to deviate from previous results only at energies above 0.3 MeV.

The results obtained in [44] and represented by boxes in Fig. 4 do not agree with the results of later measurements reported in [42] and involve comparatively large errors. The results from [42] seem more reliable, and it would be reasonable to rely on them at the present time. Among theoretical calculations, those in [36] on the basis of the cluster model and those in [37] on the basis of the resonating-group method are worthy of note. For the S factor at zero energy, they yielded 100 and 98(6) eV b, respectively. In addition, the value of $S(0) = 97.4(10)$ eV b was obtained in [33].

Thus, one can see that our calculations of the S factor for ^{3}H^{4}He radiative capture describe quite well experimental data from [42] at energies below 0.5 MeV and that, at 10 keV, these calculations lead to an S-factor value that, within the errors, agrees with the extrapolation of the data from that experiment to zero energy. It is noteworthy that our previous calculations of this S factor lead to the value of

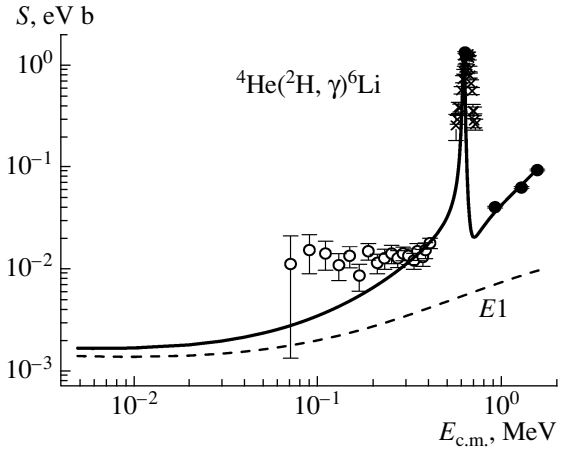

Fig. 6. Astrophysical S factor for ^{2}H^{4}He capture. The closed circles, crosses, and open circles stand for experimental data from [52], [53], and [54], respectively. The curves represent the results of the calculation with the parameters of the potentials for the ground states from Table 2.

87 eV b [13]. One may attribute this discrepancy to an approximate character of the bound-state potential, which led to a binding energy precise to within several keV units.

In Fig. 5, the solid curve represents the results obtained by calculating the astrophysical S factor for ^{3}He^{4}He capture at energies of up to 15 keV. The displayed experimental data were borrowed from [45–49]. The calculated curve agrees best of all with the results reported in [46, 47] and obtained recently at energies below 200 keV and with part of the data from [49] at energies below 0.5 MeV. At the energy of 20 keV, our calculation yielded the S-factor value of 0.593 keV b. For the sake of comparison, we present various experimental extrapolations to zero energy: 0.54(9) keV b [41], 0.550(12) keV b [50], 0.595(18) keV b [45], 0.560(17) keV b [46], 0.550(17) keV b [47], and 0.567(18) keV b [51]. For this S factor, the values of 0.56 and 0.5(3) keV b were obtained on the basis of, respectively, the cluster model [36] and the resonating-group method [37]. Recently, the analysis of various experimental data in [35] yielded the values of $S(0) = 0.610(37)$ keV b and $S(23\ \text{keV}) = 0.599(36)$ keV b, which are in good agreement with our present results.

If, in just the same way as in the case of the preceding system, one takes into account only transitions from scattering S waves to the ground and first excited states, then, at 20 keV, there arises the value of 0.587 keV b, which is virtually identical to the above value of 0.593 keV b. In Fig. 5, the results of the calculation of the S factor are represented by the dashed curve. It deviates only slightly from the results obtained previously with allowance for transitions from S and D waves.

From the results obtained in recent years, one can see that the S factor at zero energy may take values in the range 0.45–0.65 keV b, and our calculated value falls within the range of uncertainties. The form of the S factor at energies below 0.5 MeV agrees quite well with data from [49] and describes new data from [46, 47] at still lower energies. We note that our previous calculations of the S factor for the ^{3}He^{4}He capture led to the value of 0.47 keV b [13]. This difference is also attributed to an approximate character of the ground-state potential [13].

In Fig. 6, the S factor calculated for the ^{2}H^{4}He capture at energies of up to 5 keV is represented by the solid curve, the contribution to it from the $E1$ process being shown by the dashed curve. The displayed experimental data were borrowed from [52–54], but, in the last case, the results were determined from the figures presented in [41]. In the energy range 5–10 keV, the value of $1.67(1) \times 10^{-3}$ eV b (or 1.67(1) eV mb) was obtained for the total calculated S factor determined by the $E1$ and $E2$ processes. In this energy range, the contribution of the $E1$ transition proved to be dominant and equal to 1.39(1) eV mb. From here, one can see that it is the $E1$ process that makes a leading contribution to the astrophysical S factor at low energies. The quoted errors in the S factor are determined by averaging over the energy interval in question, where it remains virtually unchanged, in contrast to what we have for other systems considered above.

The results presented in [41] and obtained by extrapolating experimental data yield the value of 1.6(1) eV mb at 10 keV. It agrees well with the value obtained here. If, however, one extrapolates only data from [54], which are quite compatible with the assumption of a linear extrapolation, this may lead to an average S-factor value greater nearly by an order of magnitude, 13 eV mb. It is worthy of note that our previous calculations of the S factor for ^{2}H^{4}He radiative capture led to the value of 1.5 eV mb [13]. This difference, albeit small as it is, is also caused by an approximate character of the bound-state potential, which could yield the binding energy to a precision of a few keV units, and, possibly, by the use of integral values in our previous calculations for the masses of interacting entrance-channel particles.

A value of 1.2(1) eV mb is presented for the S factor at zero energy in the theoretical calculations reported in [29]. This value corresponds to the asymptotic normalization constant equal to 2.4, the constant extracted from experimental data [28, 55] being 2.32(11). However, the value obtained in calculations for the asymptotic normalization constant, in terms of

which one evaluates the S factor, ranges between 1.6 and 2.8; therefore, the S factor may also take values changing nearly within a factor of two. The existing ambiguity in experimental data and theoretical results presently gives no way to draw a definitive conclusion on the value of the S factor for ^{2}H^{4}He radiative capture at zero energy and on its behavior in the region above the resonance at low energies.

CONCLUSIONS

Thus, the classification of orbital states according to Young's diagrams makes it possible to construct interaction potentials that describe directly both elastic-scattering phase shifts and basic features of bound states for the nuclei being considered. In contrast to what we have for lighter nuclear systems [7, 8], this appears to be possible owing to the absence of mixing of bound states in Young's diagrams and to a greater degree of clustering of these nuclei in the ^{3}He^{4}He, ^{3}H^{4}He, and ^{2}H^{4}He cluster channels [9, 13].

It is precisely the classification of orbital states according to Young's diagrams that makes it possible to determine the number of forbidden states and, hence, the depth of the partial-wave potential that describes a specific phase shift. The phase-shift shape extracted from experimental differential cross sections makes it possible to fix the width of such a potential quite unambiguously. Thereby, the methods used here to derive the shape and depth of intercluster interactions provide the possibility for getting rid of a discrete and a continuous ambiguity that complicate the choice of potential parameters in the usual optical model.

In summary, the potential cluster model considered in the present study furnishes a solid conceptual framework for adequately describing, on the basis of unified potential parameters, not only phase shifts and properties of the ground states but also the latest experimental data on the astrophysical S factors for ^{3}He^{4}He and ^{3}H^{4}He radiative-capture processes and for obtaining acceptable values for them at zero energy.

As to the ^{2}H^{4}He system for the ^{6}Li nucleus, there are presently no sufficiently precise experimental data for this system at low energies. They are required at least in the energy range 70–500 keV but with experimental errors smaller than those in [54]. This will be helpful in drawing some specific conclusions on the shape and magnitude of the S factor at low and zero energies.

REFERENCES

1. I. M. Kapitonov, B. S. Ishkhanov, and I. A. Tutyn, *Nucleosynthesis in the Universe* (Librokom, Moscow, 2009) [in Russian]; http://nuclphys.sinp.msu.ru/nuclsynt.html
2. G. Imbriani, in *Proc. of the 3rd Eur. Summer School on Experimental Nuclear Astrophysics, S. Tecla (Catania), Sicily, Italy, Oct. 2–9, 2005.*
3. A. Caciolli et al., Eur. Phys. J. A **39**, 179 (2009).
4. S. B. Dubovichenko, Izv. Vyssh. Uchebn. Zaved., Ser. Fiz. **52** (3), 68 (2009); S. B. Dubovichenko and A. V. Dzhazairov-Kakhramanov, Uzbek. Phys. J. **10**, 364 (2008).
5. O. F. Nemets, V. G. Neudatchin, A. T. Rudchik, Yu. F. Smirnov, and Yu. M. Tchuvil'sky, *Nucleon Clusters in Nuclei and Many-Nucleon Transfer Reactions* (Nauk. Dumka, Kiev, 1988) [in Russian].
6. V. I. Kukulin, V. G. Neudatchin, and Yu. F. Smirnov, Fiz. Élem. Chastits At. Yadra **10**, 1236 (1979) [Sov. J. Part. Nucl. **10**, 492 (1979)].
7. V. G. Neudatchin, A. A. Sakharuk, and Yu. F. Smirnov, Fiz. Élem. Chastits At. Yadra **23**, 479 (1992) [Sov. J. Part. Nucl. **23**, 210 (1992)]; V. G. Neudatchin, B. G. Struzhko, and V. M. Lebedev, Fiz. Élem. Chastits At. Yadra **36**, 889 (2005) [Phys. Part. Nucl. **36**, 468 (2005)].
8. S. B. Dubovichenko and A. V. Dzhazairov-Kakhramanov, Eur. Phys. J. A **39**, 139 (2009); S. B. Dubovichenko, V. G. Neudatchin, A. A. Sakharuk, Yu. F. Smirnov, Izv. AN SSSR, Ser. Fiz. **54**, 911 (1990); V. G. Neudatchin, A. A. Sakharuk, and S. B. Dubovichenko, Few-Body Syst. **18**, 159 (1995).
9. S. B. Dubovichenko, *Properties of Light Nuclei in the Potential Cluster Model* (Daneker, Almaty, 2004) [in Russian].
10. V. G. Neudatchin and Yu. F. Smirnov, *Nucleon Clusters in Light Nuclei* (Nauka, Moscow, 1969) [in Russian].
11. S. B. Dubovichenko and A. V. Dzhazairov-Kakhramanov, Yad. Fiz. **58**, 635, 852 (1995) [Phys. At. Nucl. **58**, 579, 788 (1995)].
12. S. B. Dubovichenko and A. V. Dzhazairov-Kakhramanov, Yad. Fiz. **56** (2), 87 (1993) [Phys. At. Nucl. **56**, 195 (1993)]; **57**, 784 (1994) [Phys. At. Nucl. **57**, 733 (1994)].
13. S. B. Dubovichenko and A. V. Dzhazairov-Kakhramanov, Fiz. Élem. Chastits At. Yadra **28**, 1529 (1997) [Phys. Part. Nucl. **28**, 615 (1997)].
14. R. J. Spiger and T. A. Tombrello, Phys. Rev. **163**, 964 (1967).
15. M. Ivanovich, P. G. Young, and G. G. Ohlsen, Nucl. Phys. A **110**, 441 (1968).
16. A. C. L. Barnard, C. M. Jones, and G. C. Phillips, Nucl. Phys. **50**, 629 (1964).
17. L. C. McIntyre and W. Haeberli, Nucl. Phys. A **91**, 382 (1967).
18. L. G. Keller and W. Haeberli, Nucl. Phys. A **156**, 465 (1970).
19. W. Grüebler et al., Nucl. Phys. A **242**, 265 (1975).

20. P. A. Schmelzbach et al., Nucl. Phys. A **184**, 193 (1972).
21. S. B. Dubovichenko, Yad. Fiz. **61**, 210 (1998) [Phys. At. Nucl. **61**, 162 (1998)].
22. D. R. Tilley et al., Nucl. Phys. A **708**, 3 (2002).
23. S. B. Dubovichenko, *Methods for Calculating the Properties of Nuclei* (Kompleks, Almaty, 2006) [in Russian].
24. D. R. Tilley, H. R. Weller, and G. M. Hale, Nucl. Phys. A **541**, 1 (1992); D. R. Tilley, H. R. Weller, and H. H. Hasan, NC 27708-0308 (Triangle Univ. Nucl. Labor., Durham, 2008).
25. http://physics.nist.gov/cgi-bin/cuu/Category'view =html&Atomic+and+nuclear.x=8&Atomic +and+ nuclear.y=12
26. G. R. Plattner and R. D. Viollier, Nucl. Phys. A **365**, 8 (1981).
27. V. I. Kukulin et al., Nucl. Phys. A **417**, 128 (1984).
28. L. D. Blokhintsev et al., Phys. Rev. C **48**, 2390 (1993).
29. L. D. Blokhintsev et al., Yad. Fiz. **69**, 456 (2006) [Phys. At. Nucl. **69**, 433 (2006)].
30. T. K. Lim, Phys. Lett. B **56**, 321 (1975).
31. M. P. Bornand et al., Nucl. Phys. A **294**, 492 (1978).
32. L. D. Blokhintsev, I. Borbely, and E. I. Dolinsky, Fiz. Élem. Chastits At. Yadra **8**, 1189 (1977) [Sov. J. Part. Nucl. **8**, 485 (1977)].
33. S. B. Igamov and R. Yarmukhamedov, Nucl. Phys. A **781**, 247 (2007).
34. C. R. Brune et al., Phys. Rev. Lett. **83**, 4025 (1999).
35. S. B. Igamov, K. I. Tursunmakhatov, and R. Yarmukhamedov, arXiv:0905.2026v3 [nucl-th].
36. K. Langanke, Nucl. Phys. A **457**, 351 (1986).
37. T. Kajino, Nucl. Phys. A **460**, 559 (1986).
38. N. A. Burkova et al., Phys. Lett. B **248**, 15 (1990).
39. W. A. Fowler, G. R. Caughlan, and B. A. Zimmerman, Ann. Rev. Astron. Astrophys. **13**, 69 (1975).
40. P. J. Mohr and B. N. Taylor, Rev. Mod. Phys. **77**, 1 (2005).
41. S. Angulo et al., Nucl. Phys. A **656**, 3 (1999).
42. C. R. Brune, R. W. Kavanagh, and C. Rolfs, Phys. Rev. C **50**, 2205 (1994).
43. G. M. Griffiths et al., Can. J. Phys. **39**, 1397 (1961).
44. U. Schröder et al., Phys. Lett. B **192**, 55 (1987).
45. T. A. D. Brown et al., Phys. Rev. C **76**, 055801 (2007); arXiv:0710.1279v4 [nucl-ex].
46. F. Confortola et al., Phys. Rev. C **75**, 065803 (2007); arXiv:0705.2151v1 [nucl-ex].
47. Gy. Gyürky et al., Phys. Rev. C **75**, 035805 (2007).
48. B. S. Nara Singh et al., Phys. Rev. Lett. **93**, 262503 (2004).
49. J. L. Osborne et al., Nucl. Phys. A **419**, 115 (1984).
50. D. Bemmerer et al., Phys. Rev. Lett. **97**, 122502 (2006); nucl-ex/0609013v1.
51. H. Costantini, arXiv:0809.5269v1 [nucl-ex].
52. R. G. H. Robertson et al., Phys. Rev. Lett. **47**, 1867 (1981).
53. P. Mohr et al., Phys. Rev. C **50**, 1543 (1994).
54. J. Kiener et al., Phys. Rev. C **44**, 2195 (1991).
55. S. B. Igamov and R. Yarmukhamedov, Nucl. Phys. A **673**, 509 (2000).

Translated by A. Isaakyan